



OPEN ACCESS

EDITED BY

Zhiqiang Yin,
Anhui University of Science and
Technology, China

REVIEWED BY

Jianguo Ning,
Shandong University of Science and
Technology, China
Runsheng Lv,
Henan Polytechnic University, China
Ningbo Zhang,
China University of Mining and
Technology, China

*CORRESPONDENCE

Ying Chen,
56724647@qq.com
Xiufeng Zhang,
415690468@qq.com

SPECIALTY SECTION

This article was submitted to
Geohazards and Georisks,
a section of the journal
Frontiers in Earth Science

RECEIVED 08 June 2022

ACCEPTED 30 June 2022

PUBLISHED 26 August 2022

CITATION

Chen Y, Wang Z, Hui Q, Zhu Z, Sun D,
Chen Y, Zhang X, Wang Z, Wang J and
Zhao J (2022), Overlying rock
movement and mining pressure in a fully
mechanized caving face with a large
dip angle.
Front. Earth Sci. 10:963973.
doi: 10.3389/feart.2022.963973

COPYRIGHT

© 2022 Chen, Wang, Hui, Zhu, Sun,
Chen, Zhang, Wang, Wang and Zhao.
This is an open-access article
distributed under the terms of the
[Creative Commons Attribution License
\(CC BY\)](https://creativecommons.org/licenses/by/4.0/). The use, distribution or
reproduction in other forums is
permitted, provided the original
author(s) and the copyright owner(s) are
credited and that the original
publication in this journal is cited, in
accordance with accepted academic
practice. No use, distribution or
reproduction is permitted which does
not comply with these terms.

Overlying rock movement and mining pressure in a fully mechanized caving face with a large dip angle

Ying Chen^{1,2*}, Zhiwen Wang¹, Qianjia Hui¹, Zhijie Zhu¹,
Dequan Sun^{2,3}, Yang Chen⁴, Xiufeng Zhang^{4*}, Zhaoyi Wang⁵,
Jian Wang⁵ and Jian Zhao⁶

¹Mining Engineering School, Liaoning Technical University, Fuxin, China, ²Engineering Laboratory of Deep Mine Rockburst Disaster Assessment, Jinan, China, ³Shandong Provincial Research Institute of Coal Geology Planning and Exploration, Jinan, China, ⁴Shandong Energy Group Co. Ltd, Jinan, China, ⁵Liangbaosi Energy Co. Ltd, Shandong Energy Group Luxi Mining Co. Ltd, Jining, China, ⁶Shandong Energy Group Luxi Mining Co. Ltd, Jining, China

The overlying rock movement and mining pressure in the fully mechanized caving face with a large dip angle were systematically investigated according to theoretical analysis, similar material simulation, numerical calculation, and field monitoring. The following conclusions were obtained: 1) the theoretical analysis showed that the roof movement characteristics at different positions of the working face are quite different. The mining pressure in the upper section of the working face is primarily controlled by the structural instability of the main roof. The stable structure of the main roof is easily formed in the middle and lower sections of the working face, and the mining pressure is mostly controlled by the collapse of the immediate roof. 2) The results of similar material simulations indicated that the height of the fracture zone in different areas of the working face is different due to the influence of a large dip angle. The height of the fracture zone formed in the upper section of the working face is significantly larger than that formed in the lower section of the working face. 3) The numerical calculation suggested that the residual coal pillar of the overlying coal seam has a certain influence on the mining pressure of the 9-301 working face, making the advanced abutment pressure in the range of 80 m close to the main gate under the coal pillar more obvious. 4) The field pressure monitoring results demonstrated that the influence range of the advanced abutment pressure close to the upper part of the working face is greater than that close to the lower part of the working face, and the peak point is closer to the mining rib. Affected by the overlying residual coal pillar, the hydraulic support resistance and the peak value of advanced abutment pressure in the lower part of the working face are greater than those in the upper part. Both the initial and periodic pressure intervals of the upper section of the working face are smaller than those of the lower section. The results of this research will provide a scientific basis for the reasonable determination of the control measures for the mining pressure.

KEYWORDS

top coal caving, large dip angle, overlying rock movement, abutment pressure, numerical calculation

1 Introduction

Based on the studies on the nearly horizontal and gentle-dip coal seam, many achievements have been obtained on the overlying strata breakage and movement characteristics and mining pressure occurrence over the large-dip coal seam working face.

Since the 21st century, due to the impact of the coal market, many countries have gradually ceased the extraction of the large-dip coal seam. For instance, Great Britain and France have already closed their coalmines; thus, the research progress on the large-dip coal seam mining is slow (Singh and Gehi, 1993; Kulakov, 1995; Wang 2014; Wu et al., 2020c). Wu et al. (2020a), Luo et al. (2021), and Zhang and Wu (2020) utilized theoretical analysis, physical modeling, and field measurements to examine the breakage law of the main roof of a large-dip coal seam working face and pointed out that the asymmetrical space is easily formed due to the roof breakage, collapse sequence, and non-uniform backfilling of the gouge into the goaf. Moreover, they proposed that the main roof breakage commences from the middle and upper parts, followed, finally, by the lower part, leading to the corresponding sequence of the working face mining pressure. Wang et al. (2015a), Wang et al. (2015b), Xiao et al. (2019), and Zhang et al. (2014) built the mechanical model of the first weighting and periodic weighting of the main roof, derived the instability judgment of the roof breakage, and stated that the sequential breakage of the strata in the dip direction is mainly responsible for the formation of the asymmetrical bearing arch within the overlying strata. Combining numerical simulation and physical modeling, Xie et al. (2019) and Xie et al. (2021) found that the stress distribution and displacement of the roof of the large-dip coal seam working face were non-symmetrical, and the roof exhibited asymmetrical “O-X”-shaped breakage.

Huang (2002) stated that during the overlying strata movement of the large-dip coal seam working face, a small voussoir beam is easily formed due to the backfilling support of the caved gouge of the immediate roof, whereas a large inclined voussoir beam is easily developed for the main roof. Chai et al. (2019), Luo et al. (2018), Wu et al. (2020b), and Zhang and Wang (2014) reported that the roof deformation over the large-dip coal seam working face is non-symmetrical with higher deformation in the upper middle part than in the lower part, and the eventual caving of the overlying strata displayed non-symmetrical distribution. Zhang et al. (2010) pointed out that the overlying strata movement of the large-dip coal seam working face is non-symmetrical, and when the overlying strata break and collapse, a non-systematical backfilling zone is formed due to the downward movement along the dipping strata. Lin et al. (2015) and Luan et al. (2015) studied the dynamic evolution of the spatial structure of the overlying strata of the large-dip coal seam

working face and pointed out that the active region of the structural movement of the main roof primarily locates in the upper section over the working face; the overlying strata structure will evolve into several main roof beams at different levels and a “non-symmetrical fractured arch”. Sun et al. (2008), Rong et al. (2012), and Xie et al. (2012) investigated the “three-zone” evolution of the overlying strata of the large-dip coal seam working face. The sequential and non-uniform breakage of the overlying strata resulted in a remarkable difference in “three-zone” evolution characteristics between the lower region and the middle and upper regions of the working face; the “three zones” are highly developed in the middle and upper regions, whereas those in the lower region are less noticeable. Wang et al. (2005), Yang et al. (2010), Cheng and Li (2009), Liu et al. (2017), Men et al. (2014), Du et al. (2020a), and Du et al. (2022) also made efforts to the overlying strata movement and structural characteristics of the large-dip coal seam mining. Xiong et al. (2022), Liu et al. (2021), and Li et al. (2020) studied mining pressure caused by coal rib spalling.

Through the monitoring and analysis of mining pressure, Gao et al. (2020) stated that the periodic weighting of the large-dip, extra-thick coal seam has an obvious sequence, and the mining pressure in the middle of the working face is more severe. Zhang (2007) concluded that the support pressure at the lower end of the large-dip coal seam working face depends on the backfilling degree of the caved rock in the lower goaf, and the support pressure at the upper end depends on the roof caving when the working face is advanced. Li and Liu (2016) analyzed the mining pressure monitoring data on the large-dip coal seam working face and found that the roof stress at the lower end is larger than that of the upper end, and the upper part of the working face is loaded earlier due to the unbalanced force on the beam. Sun (2015) established a multi-section numerical model along the dip direction of the large-dip coal seam working face and obtained the distribution characteristics of the abutment pressure and the damage range of the plastic zone in the upper, middle, and lower parts of the working face in the dip direction. Yin et al. (2010), Qin et al. (2015), and Wang (2017) pointed out that the support load distribution and the weighting distance of the large-dip coal seam working face are different in the dip direction and found that the weighting period and distance were larger in the lower part than those in the upper part. Song et al. (2018) studied the mining pressure occurrence in the fully mechanized caving working face with a large dip angle and thick coal seam and obtained the mining pressure evolution of the upper, middle, and lower parts of the roof. Through the analysis of mining pressure monitoring data and numerical simulation, Xing et al. (2018) pointed out that mining pressure occurs at both ends of the working face with the mining height along the dip direction of the working face before the middle part. Zhu et al. (2014) discussed the mining pressure in the

TABLE 1 Roof and floor of the working face.

Roof and floor	Lithology	Thickness(m)
Main roof	Sandy mudstone	6–9
Immediate roof	Limestone	5–7
Immediate floor	Mudstone	1–2
Main floor	Fine sandstone	1–3

fully mechanized caving working face of soft coal seams with large dip angles and pointed out that the mining pressure in the upper, middle, and lower sections of the working face gradually weakened, and the pressure at both ends comes later than that at the middle.

Taking the 9-301 fully mechanized top coal caving working face with a large dip angle and extra-thick coal seam as the object, the overlying rock movement and mining pressure are systematically investigated by the use of theoretical analysis, similar simulation experimentation, numerical calculation, and mining pressure monitoring.

2 Field conditions

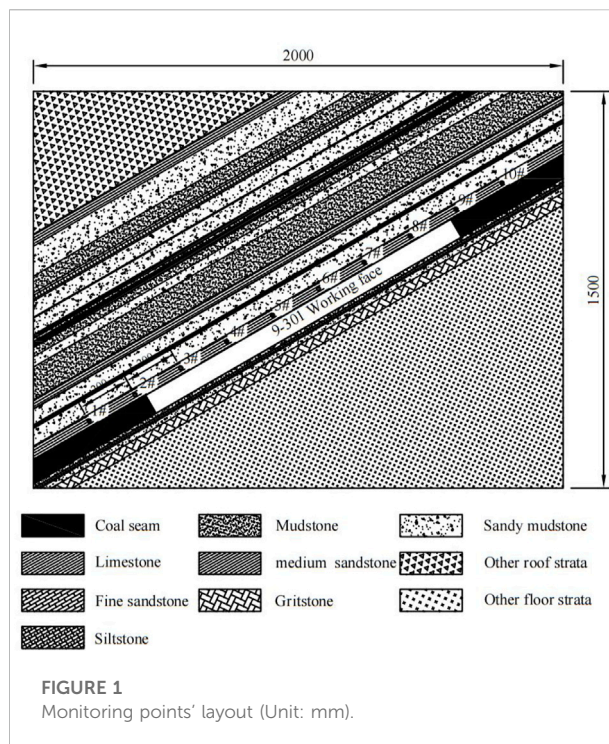
The thickness of the No. 9 coal seam in a coal mine is 10.8–12.4 m, with an average thickness of 11.8 m. The dip angle is 26°–34°, and the proctor's coefficient f is 1. The upper distance from the No. 5 coal seam is 40.90–56.15 m, with an average distance of 50.63 m. The coal seam structure is complex, containing 1–4 interlayers of gangue; the thickness of the gangue is 0.10–0.38 m; and the gangue is mostly carbonaceous mudstone.

The 9-301 working face adopts the fully mechanized top coal caving, mining the overall height at one time, with a mining height of 3.2 m, the top coal caving thickness of 8.6 m, and a mining/caving ratio of 1:2.69. The caving interval is “two cuttings and one caving,” and the caving method is single-round sequential caving. The inclined length of the working face is 200 m, and the advancing length of the strike is 2002 m. The depth of the working face is 435–540 m. The roof and floor of the working face are reported in Table 1.

3 Analysis of overlying rock movement characteristics in coal seam mining with a large dip angle

3.1 Analysis of movement characteristics of immediate roof strata

The collapse of the immediate roof of the fully mechanized top coal caving face with a large dip angle is different from that in



a horizontal (or near horizontal) coal seam. Along the inclination and strike of the working face, the collapse state and structure of the immediate roofs are quite different.

With the release of top coal, the immediate roof loses its support and reaches the strength limit under the action of the overburden rock layer. Under the condition of a large dip angle, the broken immediate roof moves down along the dip of the working face, resulting in the accumulation of gangue in the lower section of the goaf. The immediate roof of the upper section of the working face will generally collapse sufficiently and move downward. The immediate roof of the middle section of the working face is usually characterized by stratification. The lower stratification can be fully caved, while different degrees of fracture and large-sized blocks can be formed in the upper stratification. Due to the filling and supporting effect of the falling gangue in the upper and middle sections, damage and falling in the lower section of the working face can only be formed in the lower stratification of the immediate roof.

The immediate roof in the upper part of the working face will form small fragments; thus, it will not form a stable bearing structure. The immediate roof in the middle of the working face will be broken into large pieces and will be arranged neatly, and it is easy to form a small structure of a “masonry beam” along the strike. Due to the filling support, the space for deformation and caving of the immediate roof in the lower part of the working face is limited; therefore, it is easier to form a “masonry arch” structure with a certain span in the lower part than in the middle part of the working face.

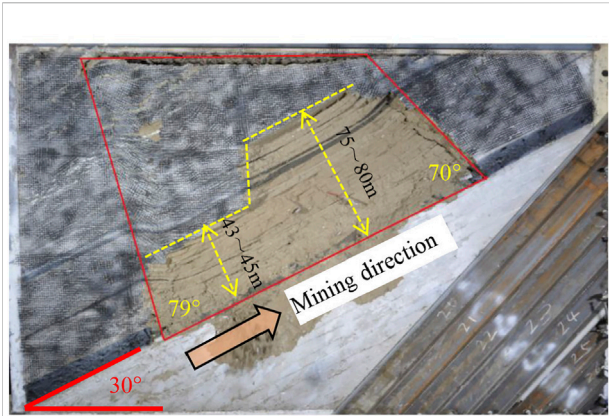


FIGURE 2 Final caving pattern of overburden.

3.2 Analysis of the main roof structure and movement characteristics

The “masonry beam” structure can be easily formed not only in the strike of the immediate roof but also in the middle and lower parts of the working face in the dip direction due to the rock gravity component (Guo et al., 2012). The “masonry beam” structure formed by the immediate roof promotes the formation of the “large structure” of the main roof.

The “large structure” formed by the main roof in the strike presents different mechanical states in the upper, middle, and lower parts of the working face. In the upper part, due to the movement and accumulation of the immediate roof falling to

the middle and lower parts of the working face, the main roof cannot be fully supported, and fracture instability occurs when the suspension length exceeds its limit deflection. Therefore, the mining pressure in the upper part of the large dip working face is affected and controlled by the instability of the main roof.

In the middle and lower parts of the working face, the main roof can maintain the structural balance and stability for a long time under the support of the immediate roof and its own structural characteristics. At the same time, it can also maintain the stability of the “masonry beam” formed by the immediate roof. Thus, the mining pressure in the middle and lower parts of the large dip working face is chiefly affected and controlled by the lower stratification collapse of the immediate roof. When the “masonry beam” formed by the immediate roof is unstable, it accelerates the damage of the main roof; thus, it affects the strength of the mining pressure.

4 Similarity experiment

4.1 Similarity parameters

The similarity method is utilized to study the overburden movement and failure process after simplifying the physical model under the ensuring similar conditions. According to the actual situation and test conditions, the following similar conditions were introduced to achieve the simulation results.

It was determined that the geometric similarity scale $\alpha_L = 150$, that is,

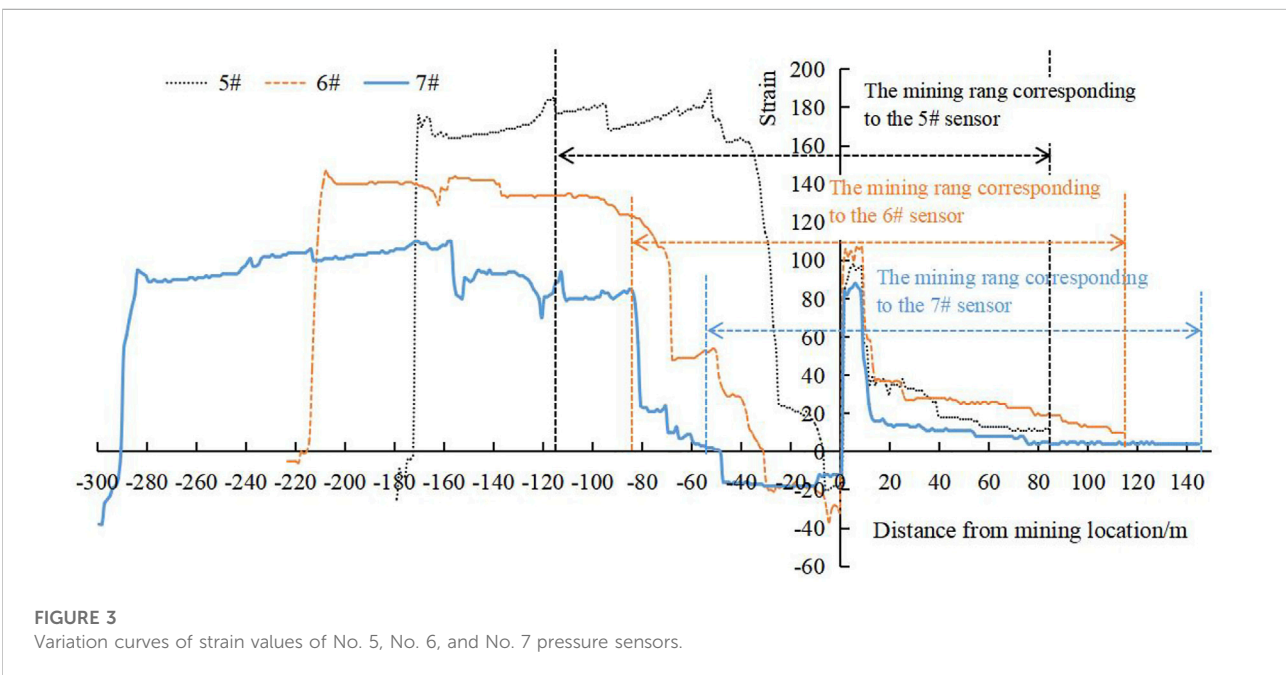


FIGURE 3 Variation curves of strain values of No. 5, No. 6, and No. 7 pressure sensors.

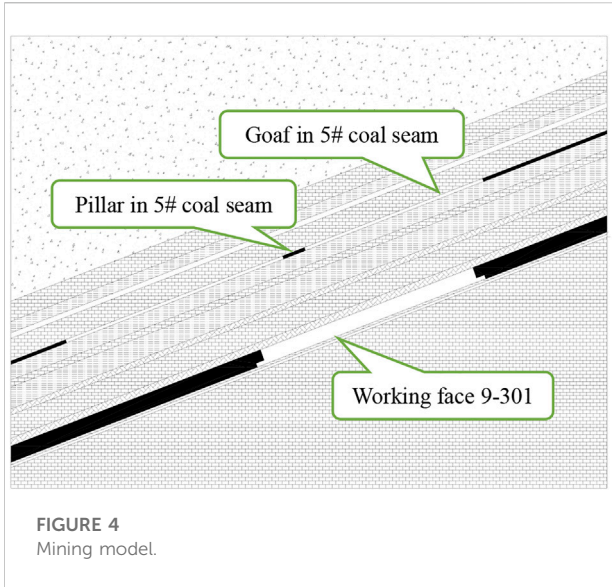


FIGURE 4 Mining model.

$$\alpha_L = \frac{L_H}{L_M} = 150, \tag{1}$$

where L_H and L_M represent the length of the prototype and the model, respectively.

Based on geometric similarity, gravity similarity is required to be constant, that is,

$$\alpha_\gamma = \frac{\gamma_H}{\gamma_M} = 1.67, \tag{2}$$

where α_γ represents the gravity similarity scale. γ_H and γ_M are the apparent densities of the rock stratum of the prototype and the model, considered to be 2.5 g/m^3 and 1.5 g/m^3 , respectively.

From geometric and gravity similarities, the stress or strength scale α_σ can be obtained as follows:

$$\alpha_\sigma = \frac{\sigma_H}{\sigma_M} = \frac{\gamma_H}{\gamma_M} \cdot \alpha_L = \frac{2.5}{1.5} \times 150 = 250, \tag{3}$$

where σ_H and σ_M are the uniaxial compressive strength of the rock stratum of the prototype and the model, respectively.

For satisfying the motion similarity, the motion of all corresponding points in the model has to be similar to that in the prototype. In other words, the speed, acceleration, and motion time of each corresponding point should be in a certain proportion. The time scale α_t is defined and obtained as follows:

$$\alpha_t = \frac{t_H}{t_M} = \sqrt{\alpha_L} = \sqrt{150} = 12.25, \tag{4}$$

where t_H and t_M represent the time of the prototype and model, respectively.

4.2 Model fabrication

The tendency model of the working face was established in a similar material experiment. The model size was length \times width \times height = $2,000 \text{ mm} \times 240 \text{ mm} \times 1,500 \text{ mm}$ (Figure 1). The model frame adopted channel steel, with two sides closed. The front and rear of the model were shaped with 240 mm-wide removable channel steel guard plates. Silica sand was selected as the aggregate, calcium carbonate and gypsum were used as cement, and mica powder was utilized for stratification. The aggregate, cement, and water were mixed evenly according to a similar proportion, and then, the mixed material was filled into the similar material model frame. In total, 10 stress monitoring points were arranged in the model (1#~10# in Figure 1). After the model was filled, it was dried for 20 days under constant temperature and humidity, and then, it was mined according to the length scale (α_L) and time scale (α_t) determined by Eqs 1, 2.

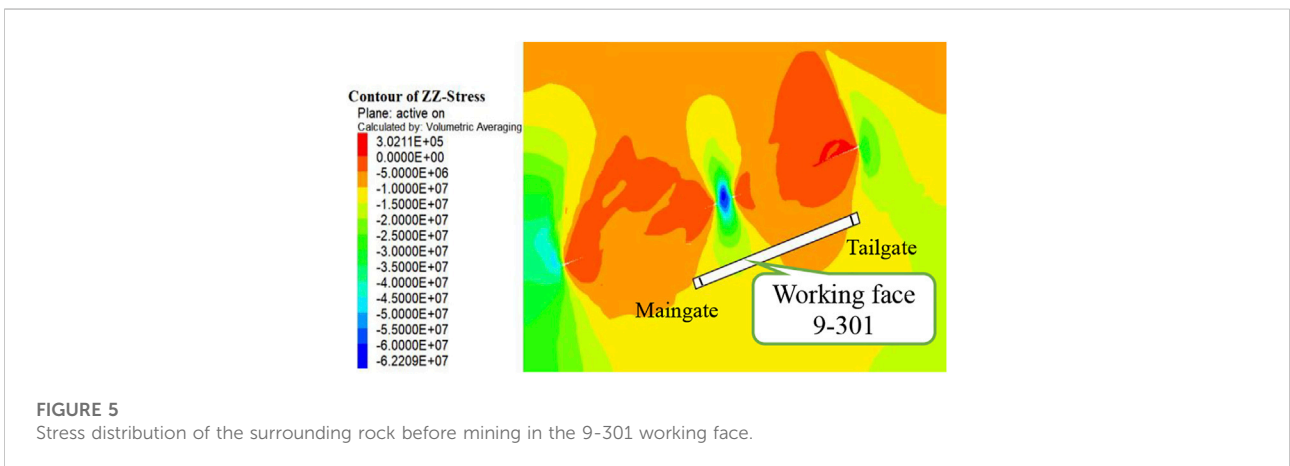
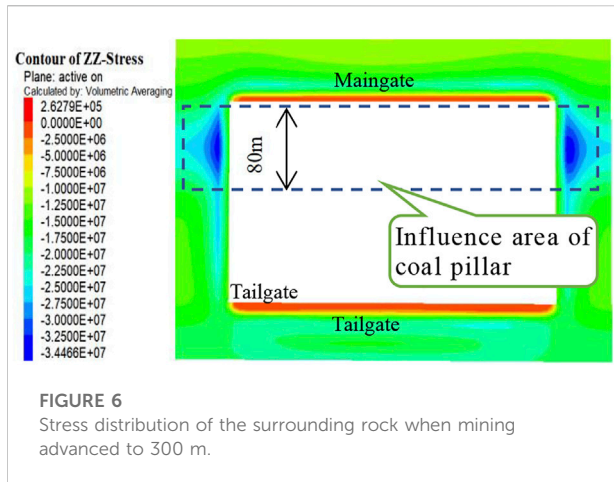


FIGURE 5 Stress distribution of the surrounding rock before mining in the 9-301 working face.



4.3 Analysis of experimental results

4.3.1 Overburden movement and failure characteristics

The geometric similarity scale chosen in the similar model is 1:150. The actual thickness of the 5# coal seam is 3.0 m, and the converted thickness in the model is 20 mm. Since the thickness is too small, the simulation mining cannot be implemented in the model. Therefore, the influence of five coal seams on the working face 9-301 is not considered in the similarity experiment.

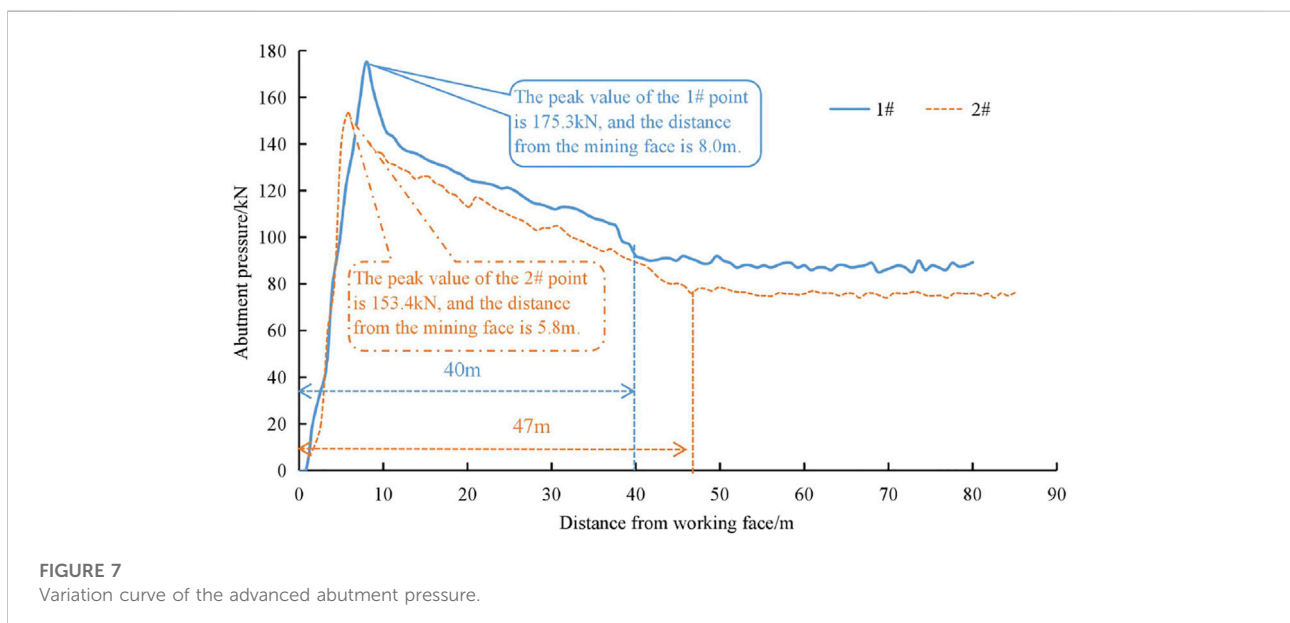
The process of the experiment was the same as the mining of coal seam. To eliminate the boundary effect, the position of 65 cm away from the model boundary was set as the initial mining position. The mining direction of the working face was

from the bottom to the top along the inclination. Considering the recovery of top coal, 93% of the thickness of the coal seam was mined in the model.

When the working face retreated to 52.5 m, the roof collapsed for the first time. The roof collapsed periodically with continuous mining. Figure 2 exhibits the final collapse form of overburden when the mining reached 200 m. The damage range of overburden caused by mining developed to the model boundary. It can be observed that because of the effect of the dip angle, the affected boundary angle of the goaf is asymmetric, the movement angle in the uphill direction is 79°, and the movement angle in the downhill direction is 70°. In the process of mining, it was found that the collapsed gangue from the upper part of the working face slipped and accumulated toward the lower part of the working face due to the influence of the dip angle, which supported and restricted the roof, causing the height of the overburden fracture zone in the lower part of the working face to be smaller than that in the upper part of the working face. The total height of the fracture zone on the working surface is 75–80 m, and the height of the fracture zone in the lower section of the working face is 43–45 m. The difference in the height of the fracture zone will lead to different mining pressures in different areas of the working face.

4.3.2 Analysis of pressure distribution in front of the working face

By embedding a BW5 micro-pressure sensor in the model, a YJZ-32A intelligent digital strain gauge was employed to monitor the real-time strain. The strain data on the sensor reflect the stress change. The strain data on some pressure



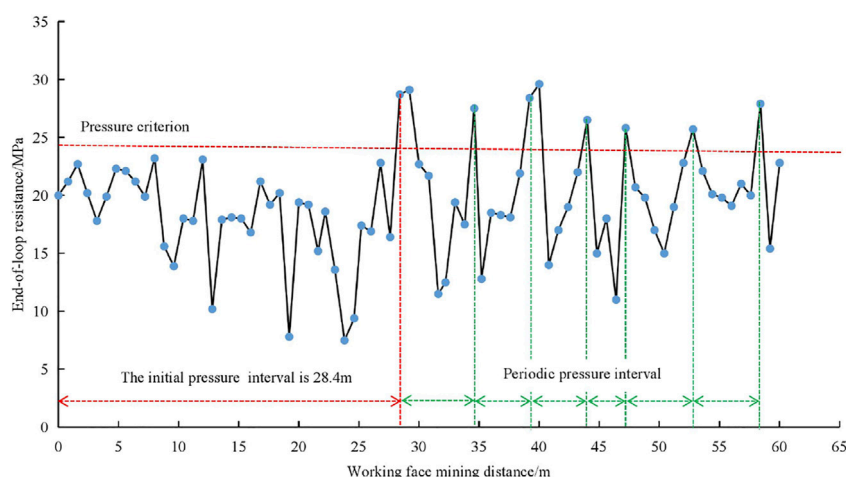


FIGURE 8
Curve of the end-of-loop resistance of the No. 15 hydraulic support.

boxes were selected, and the monitoring curve was drawn (Figure 3). The variation in the strain value of the sensor was utilized to qualitatively reflect the change in stress in the roof of the working face. The variation curves of the No. 5, No. 6, and No. 7 sensor strain values with the movement of the mining location are displayed in Figure 3. As can be observed from the figure, the strain value of the sensor gradually became larger as the mining location approached the sensor. When the position of mining was 5–7 m away from the sensor, the strain value was the largest. After that, the strain value of the sensor started to decrease. When the mining position passed through the sensor, with subsidence deformation and stress unloading of the roof, the strain of the sensor rebounded and showed a negative value. After some distance behind the mining position, the strain value of the sensor began to rise again. This means the rock stratum collapsed and recompacted, and the sensors were loaded again. When the sensors at different positions were loaded again, the distance behind the mining position and the magnitude of stress (reflected by the

magnitude of strain value) were different. With the mining of the working face from the bottom to top, the starting point of the sensor was farther and farther away from the mining position, and the No. 5, No. 6, and No. 7 sensors lagged behind the mining position by 10 m, 31 m, and 51 m, respectively. After mining, with the increase in model placement time, the strain value of sensors at each position tended to become stable after reaching a certain value. The closer to the lower part of the coal seam, the greater is the strain value (i.e., the greater the bearing stress). The experimental data indicated that the activity of the roof near the lower part of the working face is weak. It will be re-loaded after a short time of adjustment, while the roof strata located at the upper part of working face are more likely to collapse with a larger range, and the new equilibrium state requires a longer adjustment time.

The No. 1, No. 2, No. 9, and No. 10 sensors were located outside the mining district (Figure 1). Except for the strain value of the No. 9 sensor changing during mining, the strain of

TABLE 2 Statistics of the abutment pressure of the working face.

Advance/m	Abutment pressure/MPa		Peak position ahead of the working face/m	Influence range/m
	Pillar	Non-pillar		
50	28.4	14.3	6.5	30
100	30.2	19.5	6.5	37
150	30.9	22.5	6.5	40
200	31.9	24.7	6.5	47
250	32.4	25.1	6.5	47
300	32.3	25.2	6.5	49

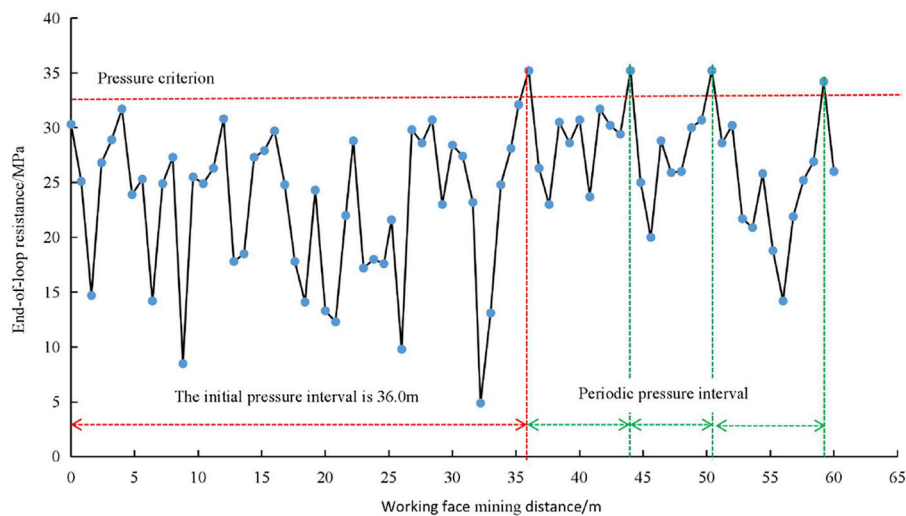


FIGURE 9
Curve of the end-of-loop resistance of the No. 40 hydraulic support.

other sensors did not change significantly (that is, mining had no impact on them). The abrupt change in the strain value of the No. 9 sensor was about 6.6 m away from the mining position, indicating that the roof strata here were affected by mining, resulting in the change in stress distribution, but the influence was small. The No. 1 and No. 2 sensors located at the bottom of the coal seam exhibited no significant change in the whole process, indicating that there was no large movement of the roof strata here, and the stress was stable. Due to the large dip angle, the mining of the working face had an impact on the side abutment pressure in the upper part of the working face, but the impact on the side abutment pressure at the lower part was not obvious.

5 Numerical simulation

5.1 Model and parameters

The numerical calculation model was established by FLAC3D. We considered the influence of the No. 5 coal seam goaf and pillar on the surrounding rock stress of the 9-301 working face (Figure 4). The model size was length \times width \times height = 500 m \times 400 m \times 250 m, and a total of 6,48,960 units and 6,83,995 nodes were established. The physical and mechanical parameters of coal and rock in the model were estimated according to the data on the mine and measured in a laboratory.

5.2 Calculation results

5.2.1 Stress distribution of the surrounding rock in the working face

Figure 5 displays the stress distribution of the surrounding rock before mining in the 9-301 working face. This figure shows that the lower part of the working face is in the stress influence area of the residual coal pillar, and the stress reaches 12–18 MPa. The upper part of the working face is located in the pressure relief area of the upper goaf, and the stress value is between 8 and 12 MPa. Figure 6 exhibits the stress distribution of the surrounding rock when mining advanced to 300 m. The working face within 80 m near the main gate is obviously affected by the concentrated stress of the coal pillar, and the abutment stress near the tailgate is small.

Table 2 shows the distribution of the advanced abutment pressure of the working face in the mining process. It can be seen that with the mining of the working face, the peak value and influence range of abutment stress gradually increase. When the working face advanced to 200 m, the peak values of the pressure under the coal pillar area and non-coal pillar area are 31.9 and 24.7 MPa, respectively. The peak point is located 6.5 m in front of the working face, and the influence range of the abutment pressure is 47 m. The mining continues in the working face, and the peak value and influence range of abutment stress tend to be stable. Affected by the coal pillar of the upper No. 5 coal seam, the lower section (near the main gate) of the 9-301 working face is affected by concentrated stress, the advanced abutment pressure is large, and the peak pressure reaches 32.4 MPa.

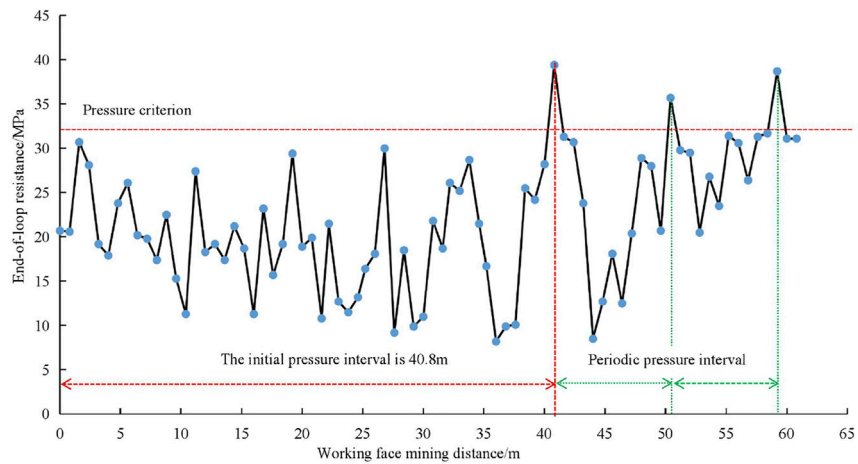


FIGURE 10
Curve of the end-of-loop resistance of the No. 65 hydraulic support.

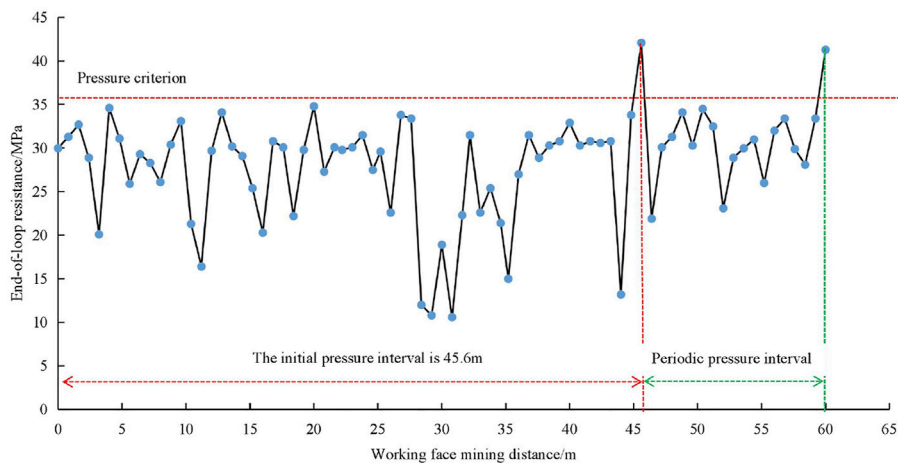


FIGURE 11
Curve of the end-of-loop resistance of the No. 90 hydraulic support.

6 Monitoring and analysis of the mining pressure

6.1 Monitoring scheme of the mining pressure

(1) The distribution and variation of the advanced abutment pressure of the working face were monitored by installing stress sensors in boreholes of the advanced coal body. To eliminate the effect of concentrated stress around the roadway, the depths of the stress sensors were determined

to be 15 m. One monitoring point was set in the main gate and another one was set in the tailgate of the 9-301 working face. A strain-type stress sensor was used on site to observe the vertical stress. The monitoring point No. 1 in the main gate of the 9-301 working face was 80 m away from the working face, and the monitoring point No. 2 in the tailgate of the 9-301 working face was 85 m away from the working face.

(2) The stress monitor installed on the hydraulic support was employed to collect the working resistance of the support in real-time. Through the filtering and statistics of the

monitoring data, the disciplines of initial and periodic pressures and the stress changes in different areas of the working face were obtained.

6.2 Analysis of the advanced abutment pressure of the working face

Statistical analysis and mapping were performed according to the monitoring data (Figure 7). As can be observed from Figure 7, the influence ranges of the advanced abutment pressure of the working face reflected by the No. 1 and No. 2 measuring points are 40 and 47 m, respectively. The position of the peak value of the measuring point No. 1 is 8 m away from the working face, with a peak value of 175.3 kN. The position of the peak value of the measuring point No. 2 is 5.8 m away from the working face, with a peak value of 153.4 kN. The measuring point No. 2 is located at the upper section along the dip of the 9-301 working face. Based on the analyses mentioned in Section 3.1 and Section 3.2, the activity of the roof in the upper section of the working face is higher than that in the lower section, owing to the large dip angle. The immediate roof and the main roof are prone to fracture and rotation deformation, resulting in structural instability. This makes the influence range of the advanced abutment pressure of the No. 1 measurement point larger and causes the peak point to occur closer to the working face. Since the measuring point No. 1 is situated within the influence range of the residual coal pillar of the overlying No. 5 coal seam, the peak value at this location is greater, which is in line with the numerical simulation results presented in Section 5.2.

6.3 Analysis of working resistance of the support of the working face

The judgment index of the periodic pressure of the working face is the sum of the average resistance at the end of the cycle of the support and its mean square deviation (Qian et al., 2021). The calculation formula is as follows:

$$\sigma_p = \sqrt{\frac{1}{n} \sum_{i=1}^n (P_{ti} - \bar{P}_t)^2}, \quad (5)$$

$$\bar{P}_t = \frac{1}{n} \sum_{i=1}^n P_{ti}, \quad (6)$$

$$P'_t = \bar{P}_t + \sigma_p. \quad (7)$$

In the aforementioned equations:

σ_p is the mean square deviation of the average value of the end of the cycle resistance;

n is the measured number of cycles;

P_{ti} is the measured value of the end-of-loop resistance (kN);

\bar{P}_t is the average value of the end-of-loop resistance (kN);

P'_t is the pressure criterion of the working face (kN).

If the measured value of the end-of-loop resistance is greater than the pressure criterion of the working face, the working face is under pressure; otherwise, it is in a non-pressure state.

A total of 101 caving hydraulic supports were arranged in the 9-301 working face, and the serial number of the supports was counted from the tailgate of the working face. The working resistance data on the No. 15, No. 40, No. 65, and No. 90 hydraulic supports were selected for statistical analysis (Figures 8–11), and the pressure criterion was employed to determine the pressure appearance of the working face. The analysis results are as follows:

- (1) The initial pressure intervals of the working face reflected by the No. 15, No. 40, No. 65, and No. 90 hydraulic supports are 28.4, 36.0, 40.8, and 45.6 m, respectively. The initial pressure at different positions of the working face is non-synchronous, which is closely related to the non-uniformity of the roof movement caused by the large dip angle of the coal seam. The gangue from the upper and middle roof of the working face moves and accumulates to the goaf at the lower part of the working face, forming support and restriction to the roof so that the roof at the lower part of the working face cannot easily fracture. Because of the lack of support of the caving gangue, the roof in the upper and middle parts of the working face breaks after the main roof reaches the limit span, resulting in the initial pressure.
- (2) The periodic pressure characteristics of each support are consistent with the initial pressure. The periodic pressure interval of the roof near the upper and middle parts of the working face (No. 15 and No. 40 supports) is about 6–9 m, and the periodic pressure interval of the roof near the lower part of the working face (No. 65 and No. 90 supports) is about 11–14 m. The phenomenon of non-synchronous pressure is also related to the large dip angle of the coal seam.
- (3) By comparing Figures 8–11, we observed that the resistance at the end of circulation of supports in the lower part of the working face (No. 65 and No. 90 supports) is generally larger than that in the upper part of the working face (No. 15 and No. 40 supports). This indicates that the stress generated by the residual coal pillar of the overlying No. 5 coal seam has a certain influence on the pressure behavior of the 9-301 working face, which is consistent with the numerical calculation results.

6.4 Application of the research results

Based on theoretical analyses, similar material simulation, numerical calculation, and field observation, several research results have been gained. The research results can be applied in the following aspects:

- (1) The results obtain the law of mining pressure interval and strength in different areas of the working face, which provided a basis for taking differentiated mine pressure control measures for different areas.
- (2) The results obtained the distribution of the advanced abutment pressure of the working face, which can be used to optimize and determine the advanced support range and select the appropriate support form.
- (3) The results obtained the movement and breaking characteristics of the roof, which can provide a basis for the selection of anti-fall and anti-skid measures for working face equipment.
- (4) The results provide an important reference for future research on the migration features of top coal.

7 Conclusion

- (1) The results of theoretical analyses demonstrated that the mining pressure in the middle and lower sections of the working face is mostly affected and controlled by the layered collapse of the immediate roof. The main roof of the upper section of the working face is more likely to be broken due to the lack of support of the immediate roof, and the mining pressure is mostly affected and controlled by falling of the main roof.
- (2) A similarity experiment was conducted with a coal seam inclination of 30°. The experiments proved that the height of the overburden fracture zone in the lower part of the working face is smaller than that in the upper part of the working face. When the pressure sensor in the roof was 5–7 m away from the mining position, the stress increased rapidly. After some distance behind the mining position, the sensor was loaded again. The closer to the upper section of the working face, the longer is the distance behind the mining position when the sensor is reloaded, indicating that the roof activity is stronger.
- (3) The numerical model of a fully mechanized coal caving face with a large dip angle was established by using FLAC3D. The calculation suggested that the residual coal pillar in the upper 5-108 face has an impact on the mining pressure of the 9-301 face, and the working face within 80 m near the main gate is obviously affected by the concentrated stress of the coal pillar. The peak values of the advanced abutment pressure in the coal pillar area and non-coal pillar area are 32.4 and 25.1 MPa, respectively. The peak point is 6.5 m in front of the face, and the influence range of the advanced abutment pressure is 47 m.
- (4) The advanced abutment pressure and hydraulic support resistance in the 9-301 working face were monitored on site. The monitoring results demonstrated that the mining pressure at different positions of the working face was asynchronous. The (initial and periodic) pressure intervals of the upper, middle, and lower sections of the working face increase successively. The influence range, peak value, and peak position of the advanced abutment pressures in the

upper and lower sections of the working face are distinct. The advanced abutment pressure in the upper section of the working face has a larger influence range, and its peak position is closer to the working face. Due to the residual coal pillar, the peak value of the advanced abutment pressure in the lower section of the working face is greater.

- (5) The results will provide a scientific basis for reasonable determination of the control measures for the mining pressure in the 9-301 working face and can also provide a reference for research on mining pressure in a fully mechanized caving face with a large dip angle.

Data availability statement

The original contributions presented in the study are included in the article/Supplementary Material; further inquiries can be directed to the corresponding authors.

Author contributions

Chen determined the structure of the manuscript, gave ideas, and conducted theoretical analysis. Wang was in charge of experiments and data analysis of similar materials. Hui was in charge of numerical modeling and calculations. Zhu performed text calibration and language polishing. Sun formulated an on-site monitoring program. Zhang was responsible for the analysis of mine pressure monitoring data. YC was in charge of data curation and graphing. ZW, JW, and JZ were responsible for monitoring instrument installation and data collection.

Funding

This work was supported by the National Natural Science Foundation of China (Grant No. 51874164), the Open Projects of the Engineering Laboratory of Deep Mine Rockburst Disaster Assessment (Grant Nos. (2020) 011 and 2021 (003)), the Major scientific and technological innovation projects in Shandong Province (Grant No. 2019SDZY02), and the Innovative Talent Support Program for Higher Education Institutions in Liaoning Province.

Conflict of interest

YC and XZ were employed by Shandong Energy Group Co., Ltd. ZW and JW were employed by Liangbaosi Energy Co., Ltd and Shandong Energy Group Luxi Mining Co., Ltd. JZ was employed by Shandong Energy Group Luxi Mining Co., Ltd.

The remaining authors declare that the research was conducted in the absence of any commercial or financial relationships that could be construed as a potential conflict of interest.

Publisher's note

All claims expressed in this article are solely those of the authors and do not necessarily represent those of their affiliated

organizations, or those of the publisher, the editors, and the reviewers. Any product that may be evaluated in this article, or claim that may be made by its manufacturer, is not guaranteed or endorsed by the publisher.

References

- Chai, J., Du, W. G., Zhang, D. D., and Lei, W. L. (2019). Study on roof activity law in steeply inclined seams based on BOTDA sensing technology. *Chin. J. Rock Mech. Eng.* 38 (09), 1809–1818. doi:10.13722/j.cnki.jrme.2018.1464
- Cheng, W. D., and Li, J. M. (2009). Stope wall rock activity law of long-wall fully mechanized caving mining on strike of steep dipping seam. *China Min. Mag.* 18 (05), 56–58
- Du, K., Li, X. F., Yang, C. Z., Zhou, J., Chen, S. J., Manoj, K., et al. (2020a). Experimental investigations on mechanical performance of rocks under fatigue loads and biaxial confinements. *J. Cent. South Univ.* 27 (10), 2985–2998. doi:10.1007/s11771-020-4523-7
- Du, K., Yang, C. Z., Su, R., Tao, M., and Wang, S. F. (2020b). Failure properties of cubic granite, marble, and sandstone specimens under true triaxial stress. *Int. J. Rock Mech. Min. Sci.* 130, 104309. doi:10.1016/j.ijrmm.2020.104309
- Du, K., Li, X. F., Su, R., Tao, M., Lv, S. Z., Luo, J., et al. (2022). Shape ratio effects on the mechanical characteristics of rectangular prism rocks and isolated pillars under uniaxial compression. *Int. J. Min. Sci. Technol.* 32 (2), 347–362. doi:10.1016/j.ijmst.2022.01.004
- Guo, D. M., Fan, J. M., Zhu, Y. L., and Zhu, X. L. (2012). Mining pressure characteristics and control technology in fully mechanized caving face in the soft and thick coal seam with a large dip angle. *Metallurgical Industry Press.*
- Gao, L. S., Zhang, E. H., Zhu, Q. J., Shi, J. J., and Wang, Y. C. (2020). Strata-pressure behavior in fully mechanized caving face with large dip angle and extra-large thickness. *J. Xi'an Univ. Sci. Technol.* 40 (04), 615–620+657
- Huang, J. G. (2002). Structural analysis for roof movement for steep coal seams. *J. China Univ. Min. Technol.* (05), 74–77.
- Kulakov, V. N. (1995). Stress state in the face region of a steep coal bed. *J. Min. Sci.* 31 (3), 161–168. doi:10.1007/bf02047661
- Li, X. M., and Liu, F. (2016). Analysis of overlying strata structure and strata behavior characteristics of stope in steep coal seam. *Coal Eng.* 48 (05), 80–83.
- Li, L., Yu, L., Zhang, S. Q., and Zhang, S. Y. (2020). Spalling mechanism of coal wall in large-angle and high-cutting coal mining face. *Coal Eng.* 52 (12), 102–107.
- Lin, D. C., Wang, G. Z., Luan, H. J., Jia, C. Y., and Dai, M. M. (2015). Experimental study on roof failure mechanism in dip mining of large inclination coal seam. *Coal Eng.* 47 (05), 98–100.
- Liu, Y. Q., Jiang, J. Q., Zhang, P. P., Gao, L., and Kong, P. (2017). Numerical simulation research on strata movement regularity of large dip angle coal seam mining. *Coal Technol.* 36 (02), 84–87. doi:10.13301/j.cnki.ct.2017.02.033
- Liu, S., Yang, K., and Tang, C. N. (2021). Mechanism and integrated control of "rib spalling: roof collapse-support instability" hazard chains in steeply dipping soft coal seams. *Adv. Mater. Sci. Eng.* 2021, 1–20. doi:10.1155/2021/5524591
- Luan, H. J., Lin, D. C., Jia, C. Y., Shi, Y. K., and Zhang, P. S. (2015). Similar simulation for overlying strata movement laws in large inclined coal seam with dip mining. *Saf. Coal Mines* 46 (09), 51–53. doi:10.13347/j.cnki.mkaq.2015.09.014
- Luo, S. H., Wu, Y. P., Liu, K. Z., Xie, P. S., and Wang, H. W. (2018). Asymmetric load and instability characteristics of coal wall at large mining height fully-mechanized face in steeply dipping seam. *J. China Coal Soc.* 43 (07), 1829–1836. doi:10.13225/j.cnki.jccs.2018.0134
- Luo, S. H., Tian, C. Y., Wu, Y. P., Xie, P. S., and Wang, H. W. (2021). Characteristics of loading and failure of overlying rock at working face advancing direction in longwall mining of steeply inclined seam. *J. China Coal Soc.* 46 (07), 2227–2236. doi:10.13225/j.cnki.jccs.2020.0379
- Men, J. G., Wang, S., Yuan, R. F., Li, X. J., Jiao, Z. H., and Peng, S. P. (2014). Study on overburden strata structure features and stress distribution law of coal pillar in inclined seam. *Coal Sci. Technol.* 42 (05), 21–24. doi:10.13199/j.cnki.cst.2014.05.006
- Qian, M. G., Xu, J. L., Wang, J. C., and Wu, Y. P. (2021). Mine pressure and rock control. *China University of Mining and Technology Press.*
- Qin, Z. C., Zhou, S. T., and Liu, M. Q. (2015). Study on stability of surrounding rock in uphill mining stope with large inclination. *Coal Eng.* 47 (07), 86–88+92
- Rong, H. R., Wang, L. G., Wang, Z. S., Zhou, D. L., and Huang, J. H. (2012). Analysis on overburden structure in the mining of deeply inclined coal seam. *Min. Res. Dev.* 32 (02), 18–21. doi:10.13827/j.cnki.kyyk.2012.02.016
- Singh, T. N., and Gehi, L. D. (1993). "State behavior during mining of steeply dipping thick seams—a case study," in The 27th international symposium on thick seam mining, Dhanbad (India), 311–315
- Song, P., Pang, X. K., and Liu, B. Z. (2018). Behavior laws of mine pressure of steep thick coal seam with stagger roadway layout in tangshan mine. *Saf. Coal Mines* 49 (12), 221–224. doi:10.13347/j.cnki.mkaq.2018.12.055
- Sun, X., Lin, C. B., and Lin, B. Q. (2008). Cracking development variation law of overlying strata over fully-mechanized coal caving mining face during exploitation process. *Saf. Coal Mines* (04), 21–24+28.
- Sun, S. L. (2015). Analysis on numerical simulation of strata behavior law of fully mechanized caving face in large dip angle. *Coal Technol.* 34 (08), 25–27. doi:10.13301/j.cnki.ct.2015.08.010
- Wang, S. R., Wang, J. A., and Dai, Y. (2005). Distinct element analysis on coal movement law and failure mechanism during mechanized top-coal caving in steep tinct seam. *J. Univ. Sci. Technol. Beijing* 27 (01), 5–8. doi:10.13374/j.issn1001-053x.2005.01.002
- Wang, J. A., Zhang, J. W., Gao, X. M., Wen, J. D., and Gu, Y. D. (2015a). Fracture mode and evolution of main roof stratum above longwall fully mechanized top coal caving in steeply inclined thick coal seam (I)—initial fracture. *J. China Coal Soc.* 40 (06), 1353–1360. doi:10.13225/j.cnki.jccs.2015.0407
- Wang, J. A., Zhang, J. W., Gao, X. M., Wen, J. D., and Gu, Y. D. (2015b). Fracture mode and evolution of main roof stratum above longwall fully mechanized top coal caving longwall coalface in steeply inclined thick coal seam (II): periodic fracture. *J. China Coal Soc.* 40 (08), 1737–1745. doi:10.13225/j.cnki.jccs.2015.0408
- Wang, H. W. (2014). *Research on evolution of stress and structural stability of surrounding rock in the longwall mining of steeply dipping seam.* Xi'an, China: Xi'an University of Science and Technology.
- Wang, C. M. (2017). Study on overburden movement and strata behavior law in fully mechanized face in thick coal seam with large angle. *Min. Saf. Environ. Prot.* 44 (04), 14–18.
- Wu, Y. P., Wang, H. W., Xie, P. S., and Zeng, Y. F. (2011). Numerical analysis on influencing factors of fractured zone height in overburden strata above high inclined seam. *Coal Eng.* 3, 63–66.
- Wu, Y. P., Liu, W. H., Xie, P. S., and Tian, S. (2020a). Stress evolution and roof breaking characteristics of surrounding rock in oblique longwall mining area of steeply dipping seam. *Saf. Coal Mines* 51 (09), 222–227. doi:10.13347/j.cnki.mkaq.2020.09.047
- Wu, Y. P., Liu, W. H., Zhang, Y. L., and Yang, W. B. (2020b). Deformation and failure characteristics of overburden in working face with steeply-angle and large mining height in the roof of interbedded coal gangue. *Min. Res. Dev.* 40 (09), 66–70. doi:10.13827/j.cnki.kyyk.2020.09.013
- Wu, Y. P., Yun, D. F., Xie, P. S., Wang, H. W., Lang, D., and Hu, B. S. (2020c). Progress, practice and scientific issues in steeply dipping coal seams fully-mechanized mining. *J. China Coal Soc.* 45 (1), 24–34. doi:10.13225/j.cnki.jccs. YG19.0494
- Xiao, J. P., Yang, K., Liu, S., and Zhou, B. (2019). Study on breaking mechanism of overlying strata in deeply inclined coal seam. *J. Saf. Sci. Technol.* 15 (03), 75–80.
- Xie, P. S., Wu, Y. P., Wang, H. W., and Ren, S. G. (2012). Study on space activity law of overburden strata above longwall coal mining face in high inclined seam. *Coal Sci. Technol.* 40 (09), 1–5. doi:10.13199/j.cst.2012.09.7.xieps.019
- Xie, P. S., Tian, S. Q., and Duan, J. J. (2019). Experimental study on the movement law of roof in pitching oblique mining area of steeply dipping seam. *J. China Coal Soc.* 44 (10), 2974–2982. doi:10.13225/j.cnki.jccs.2019.0602
- Xie, P. S., Zhang, Y. Y., Zhang, Y. L., Chen, J. J., Zhang, X. B., and Duan, J. J. (2021). Instability law of the coal-rock interbedded roof and its influence on supports in large mining height working face with steeply dipping coal seam. *J. China Coal Soc.* 46 (2), 344–356. doi:10.13225/j.cnki.jccs.xr20.1866

- Xing, D. S., Wang, L. G., and Liu, X. M. (2018). Mine pressure behavior of fully mechanized mining face with large mining height for steeply dipping coal seam. *Min. Metallurgical Eng.* 38 (05), 16–19+24.
- Xiong, Y., Kong, D. Z., Yang, S. L., Wu, G. Y., Zuo, Y. J., and Cheng, Z. B. (2022). Cloud model identification of coal face stability in steeply inclined working faces. *China Saf. Sci. J.* 32 (03), 144–151. doi:10.16265/j.cnki.issn1003-3033.2022.03.020
- Yang, Z. M., Zhang, J. H., Lai, X. P., and Lv, Z. H. (2010). Localized character of strata movement for complicated super-thick water-rich coal seam with large mining height. *J. China Coal Soc.* 35 (11), 1868–1872. doi:10.13225/j.cnki.jccs.2010.11.019
- Yin, G. Z., Li, X. S., and Guo, W. B. (2010). Photo-elastic experimental and field measurement study of ground pressure of surrounding rock of large dip angle working coalface. *Chin. J. Rock Mech. Eng.* 29 (S1), 3336–3343.
- Zhang, Y. X., and Wang, K. (2014). Roof broken features at fully mechanized caving mining stope in steep inclined and specially thick seam. *Saf. Coal Mines* 45 (07), 187–191. doi:10.13347/j.cnki.mkaq.2014.07.056
- Zhang, H., and Wu, Y. P. (2020). Timing failure mechanism of basic roof of large mining height stope in steeply dipping coal seam. *Saf. Coal Mines* 51 (03), 211–215. doi:10.13347/j.cnki.mkaq.2020.03.045
- Zhang, Y. L., Li, K. F., and Ren, S. G. (2010). Overlying strata movement property of fully mechanized caving mining in steep inclined seam. *J. Xi'an Univ. Sci. Technol.* 30 (02), 150–153. doi:10.13800/j.cnki.xakjdxsb.2010.02.010
- Zhang, C. L., Zhang, S. Q., Zhao, J. J., Li, Z. F., and Ma, Y. (2014). Law of overburden strata above longwall coal mining face in high inclined seam based on FLAC3D. *J. Liaoning Tech. Univ. Nat. Sci.* 33 (06), 736–740. doi:10.3969/j.issn.1008-0562.2014.06.004
- Zhang, L. M. (2007). Research on ground behavior law of fully mechanized caving mining face in deep inclined seam of Wangjiashan Mine. *Coal Sci. Technol.* (12), 22–26. doi:10.13199/j.cst.2007.12.26.zhanglm.008
- Zhu, X. L., Yang, R. S., Cai, Z. Y., and Qi, H. J. (2014). Study on strata pressure behavior features of fully-mechanized top coal mining in soft large inclined angle seam. *Coal Sci. Technol.* 42 (05), 25–28. doi:10.13199/j.cnki.cst.2014.05.007